ELSEVIER

Computational Materials Science 25 (2002) 193–199

COMPUTATIONAL MATERIALS SCIENCE

www.elsevier.com/locate/commatsci

Computation of deformation textures in copper with equilibrium in small grain neighbourhoods

M. Schurig *, A. Bertram

Institut für Mechanik, Otto-von-Guericke-Universität Magdeburg, 39106 Magdeburg, Germany

Abstract

The homogenization problem for polycrystalline materials is discussed with copper as an example. Crystallographic slip theory, anisotropic elasticity and a viscoplastic flow rule are used on the crystallite level. A representative volume element is modeled by finite elements and the resulting texture is compared to the elastic–plastic Taylor–Lin model and a second finite element model that restricts equilibrium to a small grain neighbourhood and tests reported by Bronkhorst et al. [Phil. Trans. R. Soc. Lond. A 341 (1992) 443]. The applicability of the last variant is also demonstrated by the decreasing deviations from stress equilibrium.
© 2002 Elsevier Science B.V. All rights reserved.

AMS: 74C20; 74Q05; 74S05
PACS: 62.20.Fe; 83.10.Ff; 83.20.Jp
Keywords: Texture; Finite plasticity; Polycrystal model

1. Introduction

The plastic deformation of a polycrystalline material is a good example for the application of mechanical theories of continua with microstructures. While from a gross viewpoint the material behaves homogeneous, detailed examination shows that the existence of several grains with individual properties can be stated.

During plastic strain the crystal orientation distribution (COD) as the major distributed property changes, and thus also the mean lattice-related properties (like overall stiffness, or heat conductivity) if the grains are anisotropic.

In a phenomenological theory it is difficult to find equations of evolution for the mean properties due to plastic deformations without considering the microstructure by a suitable homogenization technique. Hence classical theories of plasticity like the Prandtl–Reuß theory of plastic flow or Hencky's deformation theory neglect this fact by assuming that the initial symmetries remain during the whole process.

On the other hand, classical microphysics-based models neglect the need for solving the field equations of continuum mechanics. The theories that give upper and lower bounds by Taylor [12] and Sachs [10], violate equilibrium or compatibility conditions by prescription of homogeneous strain and stress fields.

* Corresponding author. Tel.: +49-391-67-12592; fax: +49-391-67-12863.
E-mail address: schurig@mb.uni-magdeburg.de (M. Schurig).

0927-0256/02/$ - see front matter © 2002 Elsevier Science B.V. All rights reserved.
PII: S0927-0256(02)00263-X

By modeling a representative volume element (RVE) of a sufficient large number of grains one can avoid the main disadvantages of Sachs and Taylor models. The price to pay is a large nonlinear system of equations that has to be solved in every load increment. The nonlinearity is geometrical due to large deformation and physical due to the constitutive equations as well.

Here we try to assure equilibrium and compatibility for at least a small neighbourhood of some grains that are modeled by finite elements, reducing the problem size.

Another approach for a neighbourhood model can be found in [11], where the compliance averages were taken over a limited neighbourhood.

2. Large deformations polycrystal model

2.1. The constitutive model

In the framework of materials with isomorphic elastic ranges [1] we use an elastic law to calculate the material stress tensor $\mathbf{S} = \mathbf{F}^{-1}\mathbf{T}\mathbf{F}^{-\top}$, $\mathbf{T}$ being the Cauchy stress tensor and $\mathbf{F}$ the deformation gradient, $\mathbf{C} = \mathbf{F}^{\top}\mathbf{F}$ the right Cauchy–Green tensor,

$$\mathbf{S} = h_{\mathrm{P}}(\mathbf{C}). \tag{1}$$

When it changes due to plastic deformation, the actual elastic function h_{P} can easily be related to a reference law h_0 by the isomorphy condition

$$h_{\mathrm{P}} = \mathbf{P}h_0(\mathbf{P}^{\top}\mathbf{C}\mathbf{P})\mathbf{P}^{\top}. \tag{2}$$

For many materials a linear elastic law is a suitable simplification of h_0 leading to

$$\widetilde{\mathbf{S}} = \widetilde{\mathbb{K}}[\widetilde{\mathbf{E}}^{G}], \tag{3}$$

where $\widetilde{\mathbb{K}}$ is the fourth order stiffness tensor. The following abbreviations have been used:

$$\widetilde{\mathbf{S}} = (\mathbf{F}\mathbf{P})^{-1}\mathbf{T}(\mathbf{F}\mathbf{P})^{-\top}, \tag{4}$$

$$\widetilde{\mathbf{E}}^{G} = \tfrac{1}{2}\big((\mathbf{F}\mathbf{P})^{\top}\mathbf{F}\mathbf{P} - \mathbf{I}\big). \tag{5}$$

The framework is suitable for single crystal plasticity, where the stress is determined by the elastic deformation of the lattice, and the elastic properties only change due to crystallographic slip. The inelastic transformation $\mathbf{P}$ maps the main axes of the elastic properties (for crystals identical with lattice vectors) belonging to the reference law onto those of a plastically deformed state. Thus it contains the information about the grains' orientation in its orthogonal part from the polar decomposition. An evolution equation for the inelastic transformation can be found based on slip kinematics. Given $\tilde{\mathbf{d}}_\alpha$ and $\tilde{\mathbf{n}}^\alpha$ the initial placement of the normalized slip direction vector and normalized glide plane normal, respectively, one finds

$$\mathbf{P}^{-1}\dot{\mathbf{P}} = -\sum_{\alpha} \dot{\gamma}_\alpha \tilde{\mathbf{d}}_\alpha \otimes \tilde{\mathbf{n}}^\alpha \tag{6}$$

for polyslip, summing over all the active glide systems.

The slip rates $\dot{\gamma}_\alpha$ of the particular slip systems can be computed by a viscoplastic regularization avoiding the well-known ambiguity in identification of the active slip systems. A simple piecewise linear overstress law of Bingham-type using the resolved shear stress and its critical value τ_α^{c}

$$\tau_\alpha = \widetilde{\mathbf{C}}\widetilde{\mathbf{S}} \cdot \tilde{\mathbf{d}}_\alpha \otimes \tilde{\mathbf{n}}^\alpha, \tag{7}$$

$$\dot{\gamma}_\alpha = \frac{1}{\eta}\big\langle |\tau_\alpha| - \tau_\alpha^{\mathrm{c}} \big\rangle \mathrm{sign}(\tau_\alpha). \tag{8}$$

Throughout the text $\mathbf{A} \cdot \mathbf{B}$ denotes the inner products.

For every slip system, an isotropic hardening law is applied. Initially the critical resolved shear stresses are assumed to be equal for every slip system. A law with self- and latent-hardening (with a ratio of 1.4) is ($\gamma = \int \sum_\beta \dot{\gamma}_\beta \,\mathrm{d}t$) [8]

$$\dot{\tau}_\alpha^{\mathrm{c}} = \left[h_{\mathrm{s}} + (h_0 - h_{\mathrm{s}})\mathrm{sech}^2\left(\frac{h_0 - h_{\mathrm{s}}}{\tau_{\mathrm{s}} - \tau_0}\gamma\right)\right] \times \dot{\gamma}_\beta \begin{cases} 1.0 & \alpha = \beta \\ 1.4 & \alpha \neq \beta \end{cases}. \tag{9}$$

The model parameters for copper have been identified in [8]. In the elastic law (3) the stiffness tensor $\widetilde{\mathbb{K}}$ for cubic material contains three independent constants, namely Young's modulus $E = 67000$ MPa, the shear modulus $G = 75000$ MPa, Poisson's ratio $\nu = 0.42$; $\eta = 2500$ MPa s^{-1}; $\tau_0 = 31$ MPa, $\tau_{\mathrm{s}} = 60$ MPa; $h_0 = 85$ MPa, $h_{\mathrm{s}} = 5.5$ MPa. The usage of a material formulation ensures

Euclidean invariance. Thus the model is capable to describe finite deformation processes without getting into conflict with objectivity requirements.

2.2. Homogenization technique

The above material model is appropriate for single crystal plasticity. In an aggregate of many—say some hundreds—crystals, the inhomogeneity has to be accounted for. For every material point the constitutive Eqs. (1)–(9) apply. In addition, the field equations of equilibrium have to be fulfilled.

The overall behaviour of an inhomogeneous medium containing many crystallites can be described by a representative volume element. By averaging all grains in the RVE the mean Cauchy stress is

$$\overline{\mathbf{T}} = \frac{1}{V}\int_V \mathbf{T}\,\mathrm{d}V. \tag{10}$$

For the mean deformation a fluctuation approach is useful [6,9]. At every material point P, the displacement is of the form:

$$\mathbf{u}(P,t) = (\overline{\mathbf{F}} - \mathbf{I})\mathbf{X}(P) + \mathbf{w}(P,t). \tag{11}$$

One can show that $\overline{\mathbf{F}}$ equals the mean deformation gradient $(1/V_0)\int_{V_0}(\mathbf{I}+\mathbf{u}\otimes\nabla)\,\mathrm{d}V$ for the displacements $\mathbf{u}(P,t)$ in (11), in each of the following three cases:

- $\mathbf{w}(\mathbf{x},t) = 0$ the fluctuation vanishes everywhere (total homogeneous case), or
- $\mathbf{w}(\mathbf{x}_b,t) = 0$ vanishes on RVE boundaries (homogeneous BC), or
- $\mathbf{w}(\mathbf{x}^+,t) = \mathbf{w}(\mathbf{x}^-,t)$ periodic on opposite boundaries of the RVE (periodic BC).

The major advantage of this approach is the possibility to implement a mean field deformation as a kind of external load and to use any numerical method to solve the equilibrium problem in the remaining fluctuation variable $\mathbf{w}(P,t)$. It has been successfully used for FEM computation of effective properties [2,8].

Using finite elements to solve the field equations of elasto-plasticity we obtain

$$\mathrm{K}(\overline{\mathbf{F}}, \widehat{\mathbb{w}}^{n+1}, \mathbf{P}_i)\left(\widehat{\mathbb{w}}^{n+1} - \widehat{\mathbb{w}}^{n}\right) = \widehat{\mathbb{f}}(\overline{\mathbf{F}}) \tag{12}$$

for the fluctuation node values $\widehat{\mathbb{w}}^{n+1}$. This nonlinear equation is valid after the $(n+1)$th load increment for the mean deformation gradient. Periodic BC are applied by elimination of the degrees of freedom rather than by application of additional constraint equations.

After equilibrium is found by an iterative scheme the update of the internal state variables takes place. A simple first order explicit Euler scheme is used for the integration of (6) and (9).

With the chosen linear tetrahedral elements every grain is discretised by five elements using eight nodes. The assembly leads to the elimination of boundary nodes to assure symmetry, and the total number of nodes for a cube-shaped RVE of $N \times N \times N$ grains is N^3.

Hence, in every load increment a nonlinear system of $3N^3$ equations has to be solved. In addition the internal state variables $\mathbf{P}$ and γ_α require integration of $5(9+12)N^3$ ODEs.

For a large number of grains, this is a time-consuming task, if the general form of (11) is used. Restricting the generality of the displacement fluctuations the interaction of neighbouring grains can be used to reduce the numerical costs of the solution.

3. The restriction to neighbourhood interaction

3.1. The Taylor–Lin model

The method introduced by Taylor [12] for a rigid-plastic solid imposes $\mathbf{w}(P,t) = 0$. Great time savings are possible, because there is no need for

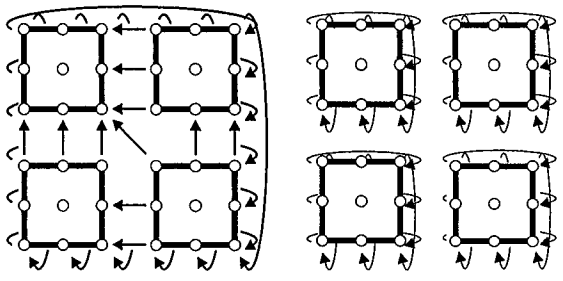

Fig. 1. Coupling of RVE parts with small neighbourhood.

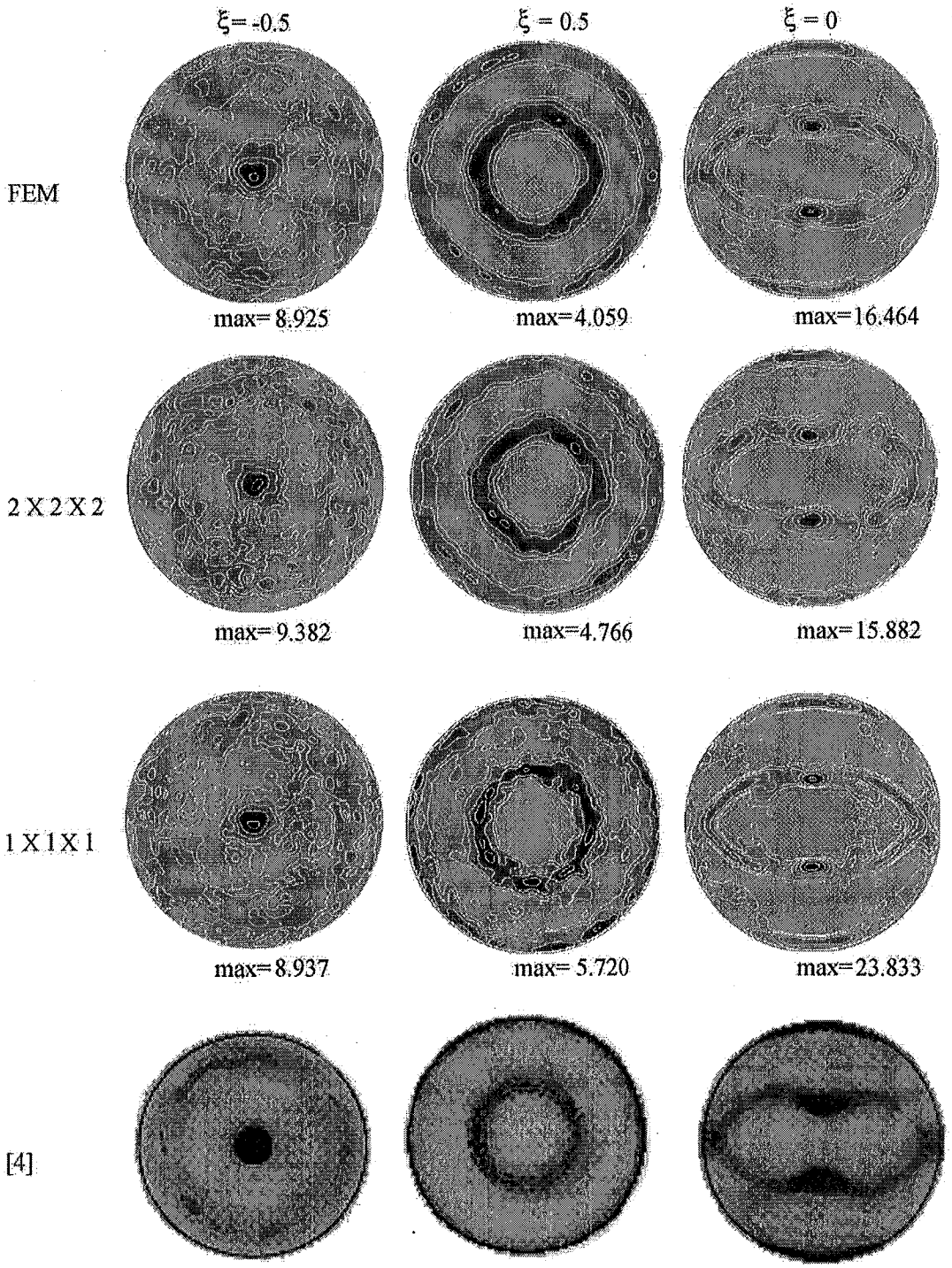

Fig. 2. ⟨1 1 1⟩ pole figures for three deformation processes. First line with FEM model of whole RVE, second with FEM model of small $2 \times 2 \times 2$ neighbourhoods, third Taylor–Lin model without grain interaction, fourth experimental results found in Bronkhorst et al. [4].

the equilibrium iteration at all. This arbitrary prescription of the displacements and the resulting reaction forces at the grain boundaries make the Taylor–Lin model loose equilibrium between neighbouring grains, while compatibility is retained.

However, it was successfully used for prediction of texture and related properties, but it is a well-known fact that the sharpness of textures predicted with the Taylor–Lin model is too high ([4], [5, p. 520]).

3.2. Small neighbourhood

Instead of the two extremes of full equilibrium iteration (the FEM based homogenization approach as shown above) and no equilibrium iteration (as in the Taylor–Lin model), the large $N \times N \times N$-grains RVE is split into smaller parts. Each part is treated individually with periodic BCs. The averaging procedure is performed for all of the parts simultaneously. At the new surfaces the coupling between the neighbouring parts is replaced by a coupling with the opposite side of the same part (see Fig. 1). This alteration of the connectivity leaves the number of DOFs and internal state variables unchanged. But the new matrix has a block diagonal structure that simplifies the solution. For every subsystem the equilibrium iteration can be solved individually. The smallest regular array possible has $2 \times 2 \times 2$ grains. It still has nine nodes and 24 DOF. Solving 64 times the nonlinear problem for 24 unknowns is equivalent of solving one problem for $8 \times 8 \times 8$ grains with 1536 unknowns, but is faster.

This procedure preserves a small neighbourhood for every grain in which equilibrium is accomplished. Compatibility is fulfilled at split surfaces in an average sense only ($\overline{\mathbf{F}} = \text{const}$), while stresses may jump.

4. Comparison of results

4.1. COD computation

The examples have been taken from the class of deformation processes with symmetric velocity gradient ($\overline{\mathbf{L}} = \dot{\overline{\mathbf{F}}}\overline{\mathbf{F}}^{-1} = \overline{\mathbf{D}}$). If the investigated medium is initially isotropic and strain rate is externally prescribed (we use $D = 0.001\ \mathrm{s}^{-1}$ for quasi-static results) this whole space can be parametrized with only one parameter ξ as shown by Böhlke and Bertram [3] using a cartesian frame,

$$\overline{\mathbf{D}}(\xi) = D \begin{bmatrix} -\frac{\sqrt{6}}{6}\xi + \frac{\sqrt{2}}{2}\sqrt{1-\xi^2} & 0 & 0 \\ 0 & \frac{\sqrt{6}}{3}\xi & 0 \\ 0 & 0 & -\frac{\sqrt{6}}{6}\xi - \frac{\sqrt{2}}{2}\sqrt{1-\xi^2} \end{bmatrix}. \tag{13}$$

For three special members of this class the COD for an aggregate of 512 grains has been determined. The strain levels reached are elongation to 145%, $\epsilon_{eq} = 0.37$ ($\xi = -0.5$), reduction to 22%, $\epsilon_{eq} = 1.5$ for simple compression ($\xi = 0.5$), and reduction to 22%, $\epsilon_{eq} = 1.8$ for plane strain compression ($\xi = 0$). Each time the calculations have been performed for the full system of 2560 elements, for the approximation by a small neighbourhood, and for the Taylor–Lin model. The visual comparison of the $\langle 1\,1\,1 \rangle$ pole figures (Fig. 2) shows similar results for each deformation process. But for larger equivalent strains (as in the $\xi = 0.5$ and 0 examples) differences in texture sharpness can be found. In each plot a fine grid and little smoothing have been used in order to make the differences visible.

The shape of the pole figures especially in the third case $\xi = 0$ coincides better with the

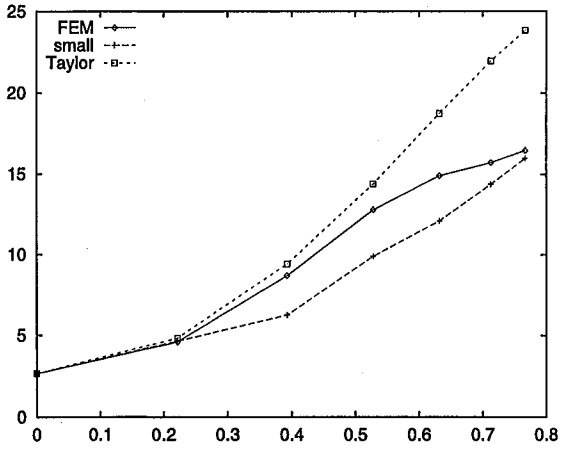

Fig. 3. Development of peak orientation density during plane strain compression process over percent thickness reduction.

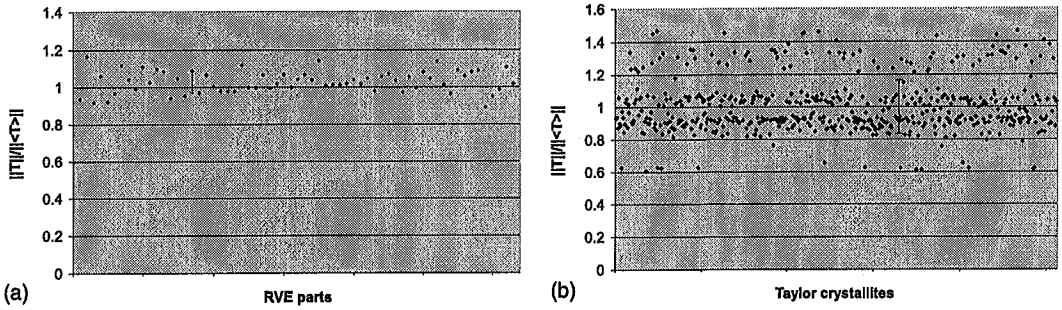

Fig. 4. Deviation from equilibrium in neighbourhoods (left) and in the crystallites of the Taylor–Lin model (right), at end of plane strain compression process. Error bars demark double standard deviation.

experiment when finite elements are used, despite the reproduction of the Brass orientation (at 3 and 9 o'clock on the circumference) is not ideal. The results for the full FEM and the $2 \times 2 \times 2$ neighbourhood are very similar.

If one takes the peak orientation density from the pole figures as an indicator (see Fig. 3) one finds that with evolving texture by strain the peak density increases. From a deformation value of approximately 50% thickness reduction the curves begin to separate showing the overestimated sharpness for Taylor–Lin model in comparison to even the smallest $2 \times 2 \times 2$ neighbourhood model.

The stresses in the RVE parts can be used for judgement of deviation from equilibrium ([7, p. 409]). In Fig. 4 the Frobenius norm of the stress averages in the $2 \times 2 \times 2$ neighbourhoods and in the crystallites of the Taylor–Lin model is plotted. The standard deviations are approximately 6% and 18%, respectively. Hence the admitted equilibrium violations at the additional internal surfaces are justified and the equilibrium is improved by much.

The computation time in an FEM program is only by part dominated by the equilibrium iteration, that can be accelerated by the reduction of stiffness matrix dimension. Other important parts are the assembly of the system matrix and integration of the internal state variables. Their speed changes when the number of grains is varied. Thus the elapsed CPU time for the small neighbourhood model drops by about 20% compared to FEM calculations of a large RVE, while the Taylor–Lin model saves approximately 80%.

5. Conclusion

For the determination of deformation textures it has been shown that at large strains the Taylor–Lin model yields too sharp textures. An FEM approach which accounts for the interaction of grains improves the situation, with certain drawbacks in the computation time.

If the grain interaction is restricted, including only a certain small neighbourhood in the equilibrium iterations, e.g. $2 \times 2 \times 2$ grains, the resulting COD shown by the pole figures are close to the solution of a FEM model of the whole RVE. Also the stress is in much better compliance with equilibrium, despite some deviations have been admitted.

Thus splitting the large problem of texture prediction into smaller uncoupled subproblems is possible. These can be solved individually, e.g. on a multi-processor workstation. This gives a hint for a simple parallelization possibility for these calculations.

References

[1] A. Bertram, An alternative approach to finite plasticity based on material isomorphisms, Int. J. Plasticity 52 (1998) 353–374.
[2] A. Bertram, Th. Böhlke, M. Kraska, Numerical simulation of deformation induced anisotropy of polycrystals, Comp. Mat. Sci. 9 (1997) 158–167.
[3] Th. Böhlke, A. Bertram, The evolution of Hooke's law due to texture development in fcc polycrystals, Int. J. Solids Struct. 38 (52) (2001) 9437–9459.

[4] C.A. Bronkhorst, S.R. Kalidindi, L. Anand, Polycrystal plasticity and the evolution of crystallographic texture in face centered cubic metals, Phil. Trans. R. Soc. Lond. A 341 (1992) 443–477.
[5] P.R. Dawson, A.J. Beaudoin, Finite element modeling of heterogeneous plasticity, in: U.F. Kocks, C.N. Tomé, H.R. Wenk (Eds.), Texture and Anisotropy, Cambridge University Press, Cambridge, 1998 (Chapter 12).
[6] R. Hill, The elastic behavior of a crystalline aggregate, Proc. Phys. Soc. A 65 (1952) 349–354.
[7] U.F. Kocks, Simulation of deformation texture development for cubic metals, in: U.F. Kocks, C.N. Tomé, H.R. Wenk (Eds.), Texture and Anisotropy, Cambridge University Press, Cambridge, 1998 (Chapter 9).
[8] Martin Kraska, Textursimulation bei großen inelastischen Verformungen mit der Technik des repräsentativen Volumenelements (RVE), Ph.D. thesis, TU Berlin, 1998.
[9] A. Krawietz, Materialtheorie, Springer, Berlin, 1986.
[10] G. Sachs, Zur Ableitung einer Fließbedingung, Z. Verein Deut. Ing. 72 (1928) 734.
[11] G.B. Sarma, P.R. Dawson, Texture predictions using a polycrystal plasticity model incorporating neighbor interactions, Int. J. Plasticity 12 (1996) 1023–1054.
[12] G.I. Taylor, Plastic strain in metals, J. Inst. Met. 62 (1938) 307–324.